Numerical prediction and reduction of pressure loss of air flow inside a sharp 90˚ elbow using turning vanes

KAHUMA LANGWANE, N. SUBASCHANDAR*
Department of Mathematics and Statistical Sciences
Botswana International University of Science and Technology
Private bag 16, Khurmela, Palapye
BOTSWANA

Abstract:- The aim of this study is to calculate the pressure loss and the effect of turning vanes on the pressure loss incurred by the flow in a duct with a 90˚ sharp elbow using numerical fluid mechanics. The main focus this study was to calculate the effects of the number of turning vanes and the length of the turning vanes on the pressure loss. Computational Fluid Dynamics calculations have been carried out using ANSYS Workbench software. Two turbulence models have been used in these calculations. They are the standard k-ε and the k-ω turbulence models. The number and length of the vanes were changed in the study to calculate their effects on pressure loss. The length of the vanes was varied from 0mm to 400mm in steps of 100mm on both sides of the bend and the number of vanes was changed from 0 to 3. It was found that a single curved turning vane can reduce the pressure loss significantly. The pressure loss does not reduce further when the length of the vanes was extended. As the number of turning vanes increased beyond one, the predicted pressure loss starts increasing. The turning vanes in duct systems can be used in industries and factories to reduce the pressure loss.

Key-words: Square duct, Sharp bend, mean velocity, Pressure loss, turbulence model, turning vanes

Received: December 30, 2021. Revised: July 12, 2021. Accepted: July 20, 2021. Published: July 27, 2021.

1 Introduction

The study of the fluid flow inside a sharp 90˚ bend is very significant in engineering applications such as heat exchangers, materials transport system and HVAC equipment. In most industrial and manufacturing units, ducts and pipes are used to transport materials. The study of the incompressible turbulent fluid flow through a two-dimensional sharp 90˚ elbow is the focus of the current research. In this report, the results of computations conducted using two turbulent models are presented. The standard k-ε and k-ω turbulence models are used in this study. In a study[1], the authors described the significance of the flow very close to the wall and the local isotropy. In the study[2], the pressure losses in bends of circular cross section was presented. The study[3] presented the results in a turbulent fluid flow inside a curved duct. In that study[3], the authors compared the results of flow inside two curved rectangular ducts with a straight duct flow. In the report[4], authors presented mean velocity profiles, energy spectrum and turbulence intensity profiles for the turbulent air flow in a duct with a smooth wall. They studied the flow inside a rectangular duct with high aspect ratio.

acting radially inwards pushes the fluid with an inward centripetal acceleration. Fluid particles, near the inside wall, have low velocities and cannot overcome the adverse pressure gradient leading to flow separation from the wall and consequently energy is transferred to smaller scales until viscous effects become important. Pressure Losses are also incurred because of the secondary flow in the radial plane of the duct due to a change in pressure in the radial direction of the duct. In a study [6] on the characteristics of open channel flows with and without turning vanes, the authors showed that the vertical vanes were very effective in reducing the pressure loss, separation of flow and the strength of secondary flows. When a flow takes place under the influence of pressure in a horizontal duct, the flow experiences a decrease in pressure in the streamwise direction because of the net energy flux into any section of the pipe is adjusted by a loss of energy due to viscous dissipation. In the fully developed duct flow, the fluid

sticks to the wall and increases to a maximum at the middle of the straight duct. If the flow is turbulent, the loss of energy is large mainly because of turbulent mixing of the fluid and the velocity profile is flatter near the centre of the duct. The velocity profile has a large gradient near the wall than the laminar flow. For the curved duct, the velocity profile is asymmetrical about the middle line of the duct. The centrifugal force changes the direction of the flow to generate secondary flows in the plane of the cross section moving the location of the maximum velocity away from the centre of the section but to some point intermediate between the centre of the duct and the outer wall of the duct. This distortion in the velocity profile is accompanied by pressure losses in the duct compared to the symmetrical velocity profile for a straight duct. Because of this feature of flow in a curved duct, a curved duct offers more resistance to the flow than a straight duct. Elbows which sharply turn fluid flow in a duct are in general used in various types of industrial equipment as well as in aircraft. These sharp turns result in total pressure losses and non-uniform velocity distributions at the bend exit, particularly past the inner part of the turn where separation frequently occurs [7].

Various methods have been reported for improving the performance of elbows designed with space limitations. The use of rows of turning vanes [8] and the use of vortex generators by[9] are examples. Turning vanes are metal devices placed inside the duct used to smoothly direct fluid inside a duct where there is a change in direction. Rows of turning vanes help the airflow negotiate the turn, and the study [9] reveals that vortex generators help to eliminate flow separation on the inside of the turn. Curved elbows though costly to manufacture, cause less energy losses than sharp elbows. Separation zones formed at the corners of the bend cause pressure losses in sharp elbows. Capturing accurately this recirculation region is difficult and this renders computation of the pressure and velocity profiles in sharp elbows difficult[10]. As the flow enters the bend region, the fluid slows down near the outer wall of the bend and flow accelerates away from the outer wall (close to the middle line of the duct) due to favourable and adverse streamwise pressure gradients. The secondary flow increases in strength as the flow goes through the bend, gathering strength as the flow reaches the exit plane of the elbow, and the faster moving fluid close to the centre of the duct is connected to the outer wall of the duct by the secondary flow. Due to the complex nature of the flow pattern inside the sharp bends, along with the difficulties of performing experimental measurements and the limitations of Computational Fluid Dynamics methods, an adequate understanding of the flow pattern inside sharp bends has not been achieved. There are some detailed studies, both experimental and numerical, on single-phase airflow and two-phase flows inside 90˚ curved bends[10,11,12]. A study reported in[5] presented extensive mean velocity measurements using Laser Doppler Anemometry (LDA) inside a square duct that had a curved bend of 90˚. They reported that the secondary flow played a major role by causing the convection of Reynolds stresses, and pushing the fluid containing high turbulent kinetic energy towards the inner wall.

Pressure forces strongly influence the mean flow and the standard turbulent eddy viscosity models cannot predict severely curved flows well, as they are inadequate to capture the generation of turbulence kinetic energy properly. Taylor et al[13] reported the importance of developing entry flow on the secondary flow development by varying the curvature ratio of the bend. Their study[13] showed that development of flow at the bend was strongly affected by the pressure gradients and crossflow convection of the secondary flow. The study[14] identified several parameters including bend radius, fluid velocity and pipe diameter that influence flow formation in the vertical pipe after the bend. They explained the influence of secondary flows and local turbulence on the flow structure and the flow recovery using computational fluid dynamics(CFD). CFD analysis is one of the key analysis methods used in engineering applications. It is non-intrusive and has been successfully used as a design tool in many engineering situations. CFD methods have been used in very complex flow situations to analyse and describe the fluid flow[15,16].

When bend ducts are used for various reasons, a penalty in the form of pressure loss is experienced. This excessive pressure drop in many situations results in increase in fan power, flow reduction and noise. The accurate calculation of pressure losses due to all pipe fittings is important in the proper design, choice of fans and for energy efficient systems[17]. A better performing system would result in significant savings in the initial investment, the operational cost and in the maintenance of the systems. Heating, Ventilation and Air Conditioning (HVAC) engineers and designers look to reduce pressure loss. In this context, turning vanes have been used to reduce the pressure loss. As the fluid changes direction in a duct, the duct walls should withstand the abrupt impact and reorient the flow to the new

path. Turning vanes help the fluid to change direction smoothly and gradually, resulting in duct walls experiencing less impact. This impact becomes important as the velocity of the fluid increases. While the turning vanes themselves add a small percentage of drag to the overall pressure loss, the amount of energy lost is insignificant compared to the energy lost in the impact because of the fluid taking an abrupt reorientation in the path.

A complete understanding of phenomena of fluids transfer is needed to the design of better performing and secure systems. In most industrial and manufacturing units, bends are often used to change the path of the flow and to establish flexibility to the system[18]. Many instruments are fixed to monitor various parameters of the machinery. It is important to accurately calculate the pressure drop in these bends[18]. In the curvature of the bend, a centrifugal force is developed as the fluid goes through the bend. The centrifugal force directs the flow towards the outer wall of the system from the centre of the curvature. The boundary layer and the centrifugal force at the wall together generate the secondary flow, consisting of two similar vortices. The superimposition of the secondary flow on the main flow along the pipe axis, which results in a streamline that has a helical shape[19]. Friction losses occur along the entire length of a duct. When the flow goes through duct fittings like sharp bends elbows, tees, diffusers, contractions, entrances and exits, the fluid may experience a change in velocity or direction of flow or both. Such changes generate flow separation and the formation of eddies and, in general, cause lot of disturbances inside the system. The disturbances thus generated may last over a considerable distance downstream of the duct fittings[20]. Pressure loss is an important parameter in the design engineering systems like coils, filters, dampers, power plants, refineries, and other HVAC systems to reduce operational and maintenance costs.

Turning vanes have been used in industry for a long time. The HVAC industry widely uses turning vanes to reorient the flow in 90˚ bends to provide the most efficient way of cooling or heating a building space. Turning vanes or guiding vanes are used in gas-turbine engine design to redirect flow to deliver optimum quantity and optimum pressure. The purposes of fixing turning vanes, one or more, in an exhaust duct with a sharp 90˚ bend are two. One reason is to reduce engine back-pressure to improve fuel economy and the second reason is to predict flow parameters in the exit region of the duct. Idelchiks Handbook of Hydraulic Resistance[21] explains the benefit of turning vanes on the flow through 90˚ bends with rounded corners. An important feature of the flow inside a duct with 90˚ elbow bends is that an eddy is formed in the corner and generates a recirculating region of fluid that opposes the principle direction of the flow. This recirculation region leads to pressure loss in the ducts with 90˚ elbow bends. It will be very beneficial if the size of this recirculation region is reduced. This current research has been extended to study of the effects of various flow conditions in ducts by varying the length of turning vane(s) and number of vanes was conducted. Turning vanes have been used to reduce pressure losses and to increase efficiency. Each engineering system is designed to deliver a specific total pressure and modifying turning vane configurations without taking these into design process will make the system function differently and the changes may make the system not supplying the fluid at the required pressure levels to all zones[21]. Research reported in the study[21] examined the pressure loss coefficients in several ductwork fittings using a commercially available CFD code, including one duct fitting with a 90˚ round elbow. From these studies Computational Fluid Dynamics method of estimating duct losses due to fittings seems to be a very good alternative to laboratory experiments to reduce design cycle time. The secondary circulation induced by flow around bends in the wind-tunnel can potentially affect the flow in the section of the tunnel where the airplane model is mounted and, hence, the measurements of various parameters. In the study[22] on pressure loss reduction in a power plant stack, the authors carried out experiments without vanes and with 30^{o} vanes. The focus of their study was mean velocity components and turbulence quantities. They reported a significant reduction of pressure loss in the presence of turning vanes[22].

The flow inside a 90˚ elbow is very complex and there is a need for research in the pressure loss reduction mechanism in such flows. From the above literature survey, it is seen that the flow in the bend has been reported extensively, both experimental and numerical studies, with focus on mean velocity profiles and turbulence profiles. Several studies have reported that pressure drop can be reduced by fixing guiding vanes in the curved elbows. However, to the best knowledge of the current authors, not many studies have been reported on pressure drop reduction inside a 90˚ sharp bend using turning vanes using numerical methods. The effects of vane lengths and vane numbers have not been studied numerically. This study was started with the idea of calculating the effect of turning vanes and length of the turning vanes on the pressure loss. Preliminary results of this study were presented in the study[23].

2 Geometry description

In this section the details of basic details of geometries studied are presented. The pressure loss reduction is achieved by introducing turning vanes at the sharp bend. The simulations are two-dimensional. The computational geometry, a two-dimensional rectangular elbow of 150mm width and consisting of a horizontal portion of 3.5m long, a sharp 90^0 elbow, and a vertical duct of 1.8m long, is shown in Fig.1. The air is admitted through the inlet of the duct at a uniform speed. The air flow throughout the duct is turbulent and fully developed at the exit. Fig. 2 shows the schematic diagram of a sharp 90^0 elbow section having one turning vane with H=0mm (H/D=0). Fig. 3 presents the schematic of the geometry with a single turning vane inside at the sharp bend. Fig. 4 shows the schematic diagram of the geometry with two turning vanes inside at the sharp bend. Fig. 5 shows the schematic diagram of the geometry with three turning vanes inside at the sharp bend. H is the vane length referring to the straight edge of the vane after the curvature and varied from 0mm to 400mm in steps of 100mm (H/D=0, 0.66, 1.25, 2 and 2.66). Vanes were placed on both sides of the bend simultaneously and each configuration was studied separately. When only one single turning vane was used, the vane was fixed equidistant from the wall as shown in Fig.2. In the case of multiple turning vanes, the turning vanes were placed equidistant from each other and from the walls as displayed on Figs.3 and 4. In all sixteen configurations were studied using Computational Fluid Dynamics. The standard k-ε and the standard k-ω turbulence models have been used in the current study. The maximum difference in the values of pressure loss predicted by the two turbulence models, as can be seen later, was less than 2 %. The contour plots of static pressure distribution inside the computational domain did not show any drastic and visible differences. Hence, most of the computational results presented will be the results obtained using the standard k-ε turbulence model. The performance of two turbulence models will be presented for pressure losses at the outlet. ANSYS workbench student ver. 16.2[24] has been used in the current study.

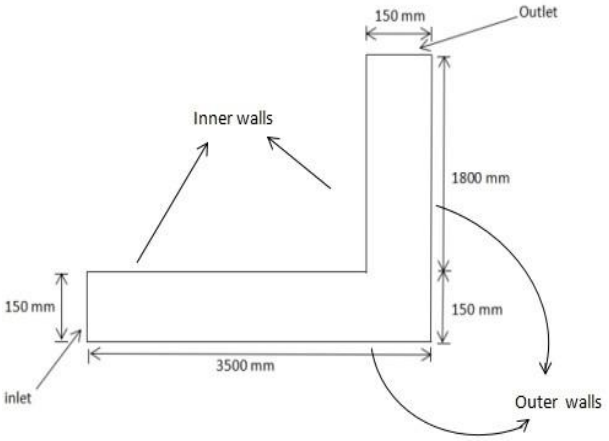

Fig. 1. Schematic diagram of a sharp 90˚ elbow without a turning vane

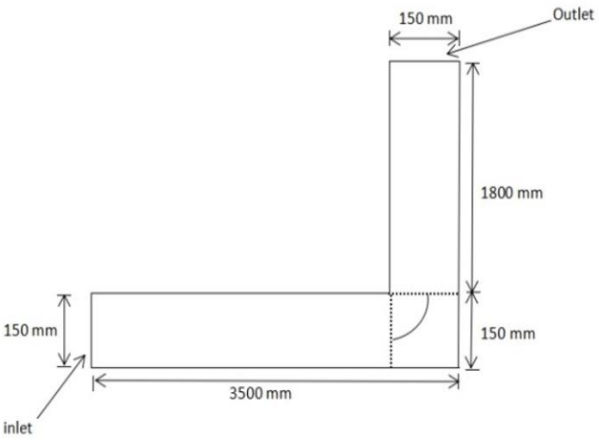

Fig. 2. Schematic diagram of sharp 90˚ elbow with one turning vane H=0mm (H/D=0)

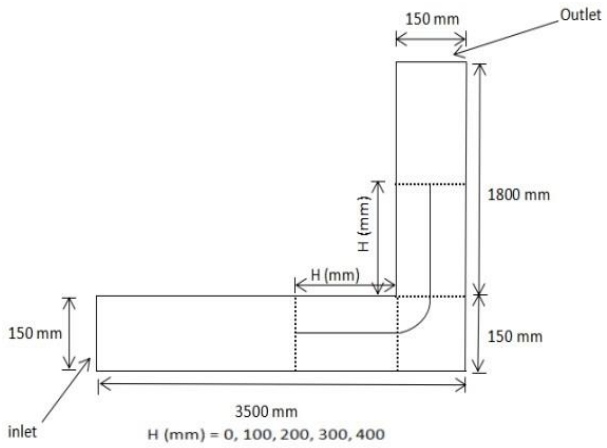

Fig. 3. Schematic diagram of sharp 90˚ elbow with one turning vane (H/D=0, 0.66, 1.25, 2 and 2.66).

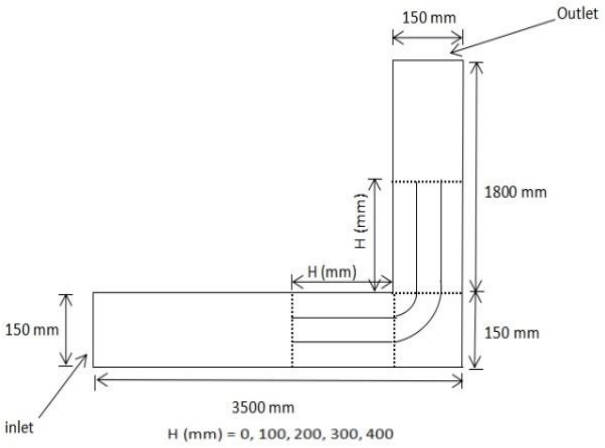

Fig. 4. Schematic diagram of sharp 90˚ elbow with two turning vanes (H/D=0, 0.66, 1.25, 2 and 2.66).

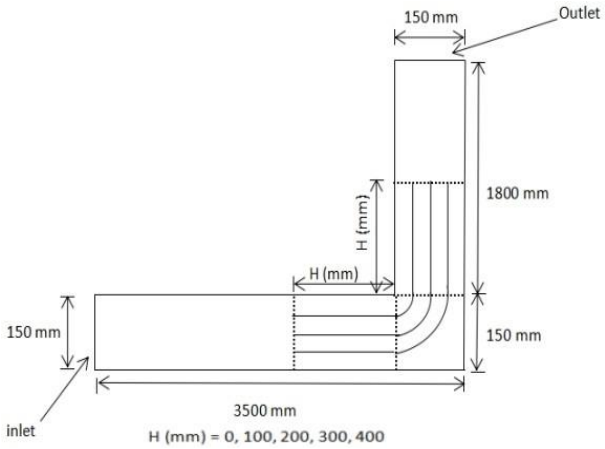

Fig. 5. Schematic diagram of sharp 90˚ elbow with three turning vanes(H/D=0, 0.66, 1.25, 2 and 2.66).

3 Mathematical Modelling

The flow studied here was incompressible, steady, two-dimensional, and turbulent. The governing equations, under above assumptions, are given below[10,25,26] :

Continuity equation:

$$\frac{\partial}{\partial x}(\rho u) + \frac{\partial}{\partial y}(\rho v) = 0 \qquad (1)$$

Momentum equation in x-direction

$$\frac{\partial}{\partial x}(\rho uu) + \frac{\partial}{\partial y}(\rho vu) = -\frac{\partial P}{\partial x} + \mu\left(\frac{\partial^2 u}{\partial x^2} + \frac{\partial^2 u}{\partial y^2}\right) - \frac{\partial}{\partial x}\left(\rho\overline{u'^2}\right) - \frac{\partial}{\partial y}\left(\rho\overline{u'v'}\right) \qquad (2)$$

Momentum equation in y-direction

$$\frac{\partial}{\partial x}(\rho uv) + \frac{\partial}{\partial y}(\rho vv) = -\frac{\partial P}{\partial y} + \mu\left(\frac{\partial^2 v}{\partial x^2} + \frac{\partial^2 v}{\partial y^2}\right) - \frac{\partial}{\partial x}\left(\rho\overline{v'u'}\right) - \frac{\partial}{\partial y}\left(\rho\overline{v'^2}\right) \qquad (3)$$

In these equations, u and v are the velocity components in the x and y directions. P is the average static pressure, ρ is the density and μ is the fluid viscosity. Flow is isothermal. Eqs. (2) and (3) are the famous Reynolds Averaged Navier-Stokes equations. $\left(\rho\overline{u'^2}\right)$, $\left(\rho\overline{u'v'}\right)$and $\left(\rho\overline{v'^2}\right)$ are the Reynolds stresses which are calculated using turbulence models. The governing equations are second order non-linear partial differential equations, not easy to get closed form solutions. The standard k-ε turbulence model has been used in the present research. In this model, turbulent kinetic energy k and its dissipation rate ε, are solved simultaneously using two transport equations. The governing equations for k and ε are given below[10,27,28]

$$\frac{\partial}{\partial t}(\rho k) + \frac{\partial y}{\partial x_i}(\rho k u_i) = \frac{\partial}{\partial x_j}\left[\left(\mu + \frac{\mu_i}{\sigma_k}\right)\frac{\partial k}{\partial x_j}\right] + G_k + \rho\varepsilon + S_k \qquad (4)$$

$$\frac{\partial}{\partial t}(\rho\varepsilon) + \frac{\partial}{\partial x_i}(\rho\varepsilon u_i) = \frac{\partial}{\partial x_j}\left[\left(\mu + \frac{\mu_i}{\sigma_k}\right)\frac{\partial \varepsilon}{\partial x_j}\right] + C_{1\varepsilon}\frac{\varepsilon}{k}(G_k) - C_{2\varepsilon}\rho\frac{\varepsilon^2}{K} + S_\varepsilon \qquad (5)$$

where G_k represents the generation of turbulent kinetic energy arising due to velocity gradients. Values of constants have been obtained experimentally and have following values.

$C_{1\varepsilon} = 1.44$, $C_{2\varepsilon} = 1.92$, $\sigma_k = 1.0$ and $\sigma_\varepsilon = 1.3$

The eddy viscosity is computed using the local values of turbulent kinetic energy and its dissipation rate and using the equation given by:

$$\mu_t = \rho C_\mu \frac{k^2}{\varepsilon} \ ,$$

where C_μ has a constant value of 0.09. The term for the production of turbulent kinetic energy G_k is defined as $G_k = -\overline{\rho u'_\imath u'_\jmath}\frac{\partial u_j}{\partial x_i}$. S_ε and S_k are the source terms.

ANSYS Workbench student version[24] uses the standard k-ω turbulence model which was developed to calculate low-Reynolds number effects and compressibility effects very accurately. The standard model k-ω turbulence model is an empirically developed model with transport equations for turbulent kinetic energy k and its specific dissipation

rate ω. ε is defined as dissipation rate per unit mass and ω is dissipation rate per unit kinetic energy. The differential equations used for the standard k-ω turbulence model are given below[29,30].

$$\frac{\partial}{\partial x_i}(\rho k u_i) = \frac{\partial}{\partial x_i}\left[\left(\mu + \frac{u_t}{\sigma_k}\right)\frac{\partial k}{\partial x_j}\right] + G_k - Y_k + S_k \quad (6)$$

$$\frac{\partial}{\partial x_i}(\rho \omega u_i) = \frac{\partial}{\partial x_i}\left[\left(\mu + \frac{u_t}{\sigma_\omega}\right)\frac{\partial \omega}{\partial x_j}\right] + G_\omega - Y_\omega + S_\omega \quad (7)$$

where G_k denotes the turbulent kinetic energy generation that arises due to gradients in the mean velocity and G_ω denotes the generation of ω defined in the same manner as the standard k−ε turbulence model. Y_k and Y_ω signify the dissipation of k and ω due to turbulence. δ_k and δ_ω are the turbulent Prandtl number (equal to 2) for k and ω, respectively.

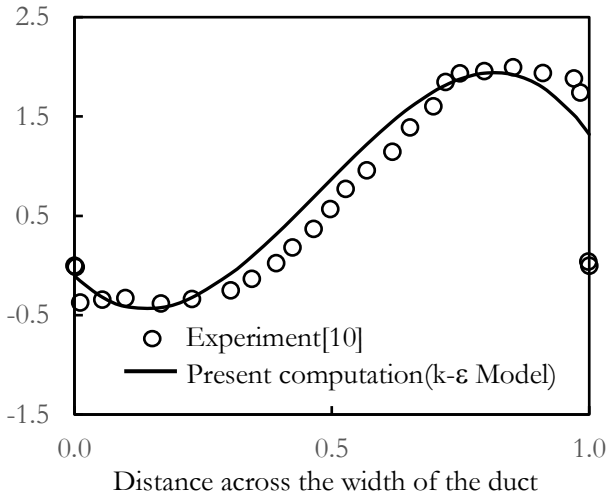

Fig. 6. Streamwise mean velocity(vertical axis) after the 90˚ sharp bend (2 duct width distance downstream of the bend)

The non-equilibrium wall function was used for both turbulence models to calculate the effects of pressure gradients by using a two-layer approach. The wall layer consists of a viscous sub-layer near the wall and a fully developed turbulent fluid layer. The turbulent kinetic energy is computed near wall cells using log-law for mean velocity that leading to accurate computation of the effects of pressure gradients[31]. The first order upwind method has been used to discretize the momentum equations, turbulent kinetic energy, and turbulence dissipation rate equations. The PREssure STaggering scheme(PRESTO) technique was used for the pressure[31,32]. The Semi-Implicit Method for Pressure-Linked Equations(SIMPLE) method was implemented for pressure-velocity interactions[31]. At the inlet, a uniform velocity condition is given. The exit was considered as a pressure outlet. On the walls the zero mean velocity condition was imposed. The computational fluid dynamics software ANSYS Workbench student version[24] has been used to solve these partial differential equations, because of its user-friendliness and capability. ANSYS software uses a finite-volume based discretization method.

4 Results and Discussion

In this section, important results of the current study are presented.

4.1 Computational model validation

The computational methodology and present modelling were validated by using following methods.

1. By carrying out a grid independence study.
2. By checking the mass flow rate at the inlet and exit.
3. By comparing the present computational results with available results in the literature.

A two-dimensional computational model as shown in Fig.1 was constructed. ANSYS Workbench student version was used for construction of the geometry in the present computations. Meshes with difference sizes in the range 105,000 to 165,000 nodes, were generated. Table 1 shows the pressure loss coefficient calculated using difference mesh sizes. It can be seen from the Table 1 that pressure loss value is not significantly different for grid 4 and grid 5. Hence all subsequent calculations were performed with mesh sizes of about 159,000. Fig. 6 shows the comparison of computed and experimental mean velocity profiles at a location after the sharp bend(2 duct width distance downstream of the bend). Measurements were made using Laser Doppler Velocity technique, inside a sharp 90° bend in a horizontal-to-vertical suction open-circuit wind tunnel system. The cross section of the test section was 150×150 (mm^2) square and was made of 10mm thick Perspex. It had a 3.5m-long straight horizontal duct. It had a sharp 90° bend and a 1.8m-long straight vertical duct. Detailed description of the set-up has been given in the reports[10,33]. It can be seen from the Fig. 6 that the computed and experimental streamwise mean velocity profiles at this location agree reasonably well, with maximum difference in the region close to the centre of the duct being less than 10%. The differences are larger near the walls.

It should be recalled here that the computational study was carried out in a two-dimensional domain whereas the experimental results presented are from the three-dimensional study. The computations were carried out by monitoring the residuals during the calculations and keeping the differences between the mass flow rates at the inlet and outlet very low. The mass flow rate difference between the inlet and the outlet is 0.001% which is very small. The iterations were stopped when all the residuals reached below 0.0001. Pressure loss coefficient was calculated using the formula below.

$$Kp(\%)=\text{Pressure loss} = (P_{in}-P_{out})/P_{in} \times 100 \quad (8)$$

Table 1. Pressure loss calculated for different grid sizes

Grid	Nodes	Kp(%)
1	109925	0.0917
2	135946	0.0926
3	140000	0.0934
4	158691	0.0939
5	163239	0.0940

4.2. Effect of Reynold number on pressure loss

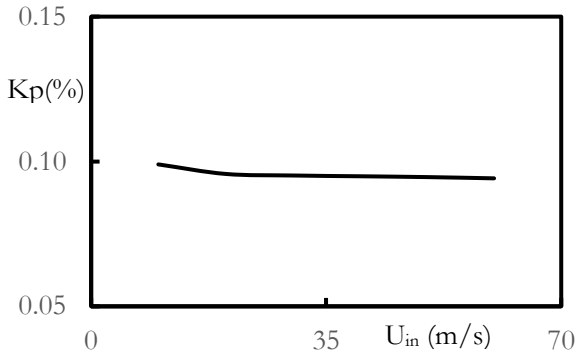

Fig. 7 Variation of pressure loss with uniform inlet velocity(Reynolds number)

Table 2 Variation of pressure loss with Reynolds number.

Uin(m/s)	Re	Kp (%)
10	97730	0.0990
20	195460	0.0957
30	293190	0.0952
40	390920	0.0949
50	488650	0.0946
60	586380	0.0942

The results for the effect of Reynolds number overthe pressure loss (Kp(%)) for a square duct with a sharp 90° bend without turning vane(s) are presented in this section. Calculations carried out using the standard k-ε turbulence model are only presented here. Reynold number of the flow was calculated using the inlet velocity and the duct width. The inlet velocity was varied between 10 m/s to 60 m/s so that the Reynolds number varied from about 97000 to about 600000. Flow can be considered to be in the high Reynolds number region for all configurations studied here. Fig 7 presents the results for the effect of inlet velocity on the pressure loss for the flow inside the duct with 90° sharp bend angle and without turning vane(s). To avoid writing large numbers on the horizontal axis to represent Reynolds number, inlet velocity was plotted on the horizontal axis. However, Table 1 presents the results for the effect of Reynolds number(also inlet velocity) on the pressure loss for the flow inside the duct with 90° sharp bend angle and without turning vane(s). From the results presented in the Fig. 7 and Table 2, it is observed that the computed pressure loss(Kp(%)) varies very slightly as the Reynolds number increases and that the pressure loss tends to a constant value as is to be expected in high Reynolds number duct flows[34]. This constant value for the pressure loss for the flow inside the duct with 90° sharp bend without turning vane(s) is 0.094 %.

4.3. Effect of vane length on pressure loss

4.3.1 CASE 1: One turning vane

The length of the turning vane was initially set to H=0mm as illustrated in Fig 2, H is the straight length after the curvature in the elbow. The lengths of the turning vanes were extended on both sides from 100 mm to 400 mm in steps of 100mm (H/D=0, 0.66, 1.25, 2 and 2.66). For each configuration computations were carried out and pressure loss was calculated. Table 3 presents the pressure loss for configurations with different vane lengths. From the Table 3 the pressure loss is lower for all configurations compared to the configuration without the turning vane. However, if the vane length is increased beyond H=0mm (H/D=0), the predicted pressure loss starts increasing. These computations reveal that there is an optimum length for the turning vane beyond which the pressure loss starts increasing reducing the benefit of lowering pressure loss. From the Table 3, the optimum length seems to be H=0mm (H/D=0). Initial the pressure loss is reduced as the flow turns smoothly because of the presence of turning vane. The large circulation zone which is observed on the bottom sharp corner is also reduced, because the presence of large recirculation zone contributes to the pressure loss. But as the vane length exceeds H=0 mm, drag is

formed along the turning vane and more recirculation zone is formed and this led to the decrease in the pressure loss.

Table 3 Computed pressure loss variation with length for one turning vane.

Configuration	Vane length (Hmm)	H/D	Kp(%)
No vane	-	-	0.0941
One vane	0	0	0.0450
One vane	100	0.66	0.0509
One vane	200	1.25	0.0562
One vane	300	2.0	0.0603
One vane	400	2.66	0.0615

4.3.2 CASE 2: Two turning vanes

Table 4 presents the results for pressure loss for configurations with different vane lengths. From Table 4, the optimum length seems to be 0 mm. These results suggest that smaller incremental length for the vanes (H) need to be considered. The computational work was then extended to find the impact of three turning vanes on 90˚ elbow. There is pressure drop reduction up to H=0 mm length. The drag start increasing when the turning vane length exceeds H=0 mm, and that will lead to increase in pressure loss.

4.3.3 CASE 3: Three turning vanes

Table 5 presents the pressure loss for configurations with different vane lengths. From the Table 5 the pressure loss is lower for all configurations compared to the configuration without the turning vane. However, if the vane length is increased, the predicted pressure loss starts increasing. These computations reveal that there is an optimum length for the turning vane beyond which the pressure loss starts increasing reducing the benefit of lowering pressure loss.

Table 4. Computed pressure loss variation with length for with two turning vanes.

Configuration	Vane length (Hmm)	H/D	Kp(%)
No vane	-	-	0.0941
Two vanes	0	0	0.0482
Two vanes	100	0.66	0.0525
Two vanes	200	1.25	0.0594
Two vanes	300	2.00	0.0649
Two vanes	400	2.66	0.065

From the Table 5, the optimum length seems to be 0 mm (H/D=0) and agrees with the case of a two turning vanes. Three turning vanes of length H=0mm show reduction in pressure loss, while the turning vane surfaces do contribute a small fraction of drag, the energy loss due to friction is not significant compared to the gains realized from minimizing the impact because of sudden change in direction. But increasing the lengths beyond H=0mm the energy loss due to friction is noticed hence pressure loss increased.

Table 5. Computed pressure loss variation with length for three turning vanes.

Configuration	Vane Length (Hmm)	H/D	Kp(%)
No vane	-	-	0.0941
Three vanes	0	0	0.0509
Three vanes	100	0.66	0.0567
Three vanes	200	1.25	0.0641
Three vanes	300	2.00	0.0706
Three vanes	400	2.66	0.0726

From the results presented in the Tables 3,4 and 5 it is seen that maximum pressure loss reduction is achieved with one vane kept at the centre of the sharp bend without extensions on either sides. If the vane length is increased, for single vane or multiple vanes, the pressure loss reduction increases reducing the benefit, but still the pressure loss is less than what it would have been the case where there were no vanes.

4.4 Effect of increasing the number of vanes

Computations were made by fixing the lengths of turning vanes and increasing the number of turning vanes.

Table 6. Computed pressure loss for different number of turning vanes (H=0mm , H/D = 0).

No. of vanes	**Kp(%)**
0	0.0941
1	0.0450
2	0.0482
3	0.0509

Table 7. Computed pressure loss for different number of turning vanes (H=100mm, H/D=0.66).

No. of vanes	**Kp(%)**
0	0.0941
1	0.0509
2	0.0525
3	0.0567

4.4.1 CASE 4: H=0mm (H/D=0.0)

In this case a short vane (H=0 mm) and thickness of 1 mm was used for all the configurations with one, two and three turning vanes as shown in the Figs 2 to 5. A comparison was made, and it is evident that as the numbers of turning vanes as they were increased the calculated pressure loss gradually decreased as displayed in Table 6. All the pressure losses under these configurations were less than the case without a turning vane. The possible cause of these results is that as more turning vanes are placed at the elbow less impact of the flow on the outer wall is achieved and hence the pressure loss.

4.4.2 CASE 6: H=100mm (H/D=0.66)

A comparison was made, and it is evident that as the number of turning vanes is increased the calculated pressure loss gradually decreased significantly as displayed in Table 7. All the pressure losses under this configuration is less than in the absence of a turning vane. However, if the vane length is increased, the predicted pressure loss starts increasing. This is because as we increase the number of turning vanes, drag due to vanes increases, this led to reduction in pressure loss.

4.4.3 CASE 7: H=200mm (H/D=1.25)

In this case a short vane (H=200 mm) and thickness of 1 mm was used for all the configurations with one, two and three turning vanes as in Figs 2 to 5. A comparison was made, and it is evident that as the numbers of turning vanes as they were increased the calculated pressure loss gradually decreased as displayed on Table 8. The pressure loss for the configuration with one the turning vane is less compared to other turning vanes. However, if the number of vanes is increased, the predicted pressure loss starts increasing. This is because as we increase the number of turning vanes drag is formed along the turning vane and more recirculation zone is formed and this leads to pressure loss.

Table 8. Computed pressure loss for different number of turning vanes (H=200mm, H/D=1.25).

No. of vanes	Kp(%)
0	0.0941
1	0.0562
2	0.0592
3	0.0641

4.4.4 CASE 8: H=300mm (H/D=2)

In this case a short vane (H=300 mm) and thickness of 1 mm was used for all the configurations with one, two and three turning vanes as in Figs 2 to 5. A comparison was made, and it is evident that as the numbers of turning vanes as they were increased the calculated pressure loss gradually decreased significantly as displayed on Table 9. However, if the vane length is increased, the predicted pressure loss starts increasing. This is because as we increase the number of turning vanes drag is formed along the turning vane and more recirculation zone is formed and this leads to pressure loss.

Table 9. Computed pressure loss for different number of turning vanes (H=300mm, H/D=2).

No. of vanes	Kp(%)
0	0.0941
1	0.0603
2	0.0649
3	0.0706

4.4.5. CASE 9: H=400mm (H/D=2.66)

In this case a short vane (H=400mm) and thickness of 1 mm was used for all the configurations with one, two and three turning vanes as in Figs 2 to 5. A comparison was made, and it is evident that as the numbers of turning vanes as they were increased the calculated pressure loss gradually decreased significantly as displayed on Table 10. However, if the vane length is increased, the predicted pressure loss starts increasing. From the above results, the one turning vane with H=0mm (H/D=0) seems to be the optimum configuration. If the number of vanes is increased beyond one and/or length of the vane(s) is increased beyond H=0mm (H/D=0), the pressure loss starts increasing, thus reducing the benefit. Figures 8 to 11 are used to display contour plots of total pressure distribution inside ducts with various configurations of turning vanes. It is seen from Fig. 8 that the pressure is very high in sharp corner of the elbow. This will be the location that will break in case of wear- out. From the Figs 9 to 11, one can see that the pressure in the corner of the elbow is gradually reduced as the number of vanes is increased.

Table 10. Computed pressure loss for different number of turning vanes (H=400mm, H/D=2.66).

No. of vanes	Kp(%)
0	0.0941
1	0.0615
2	0.0650
3	0.0726

4.5. Effect of number of vanes on separation length on the inner wall

Flow separation occurs when the flow is slowing down and the pressure is increasing, after the fluid goes over the thickest part of the object or passing through a diverging passage. The separated flow develops a constant pressure on the surface after separation instead of pressure increasing monotonically if the flow were still attached. In the current flow, the flow separation on the inner vertical wall is studied.

Table 11. Separation length on the inner vertical wall.

No. of vanes	$(S_L)/D$
0	2.91
1	1.67
2	1.31
3	1.01

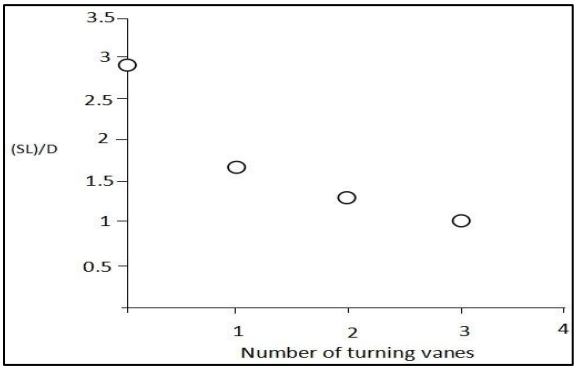

Fig. 8. Effect of number of vanes on the separation length on the inner vertical wall (vanes H=0mm).

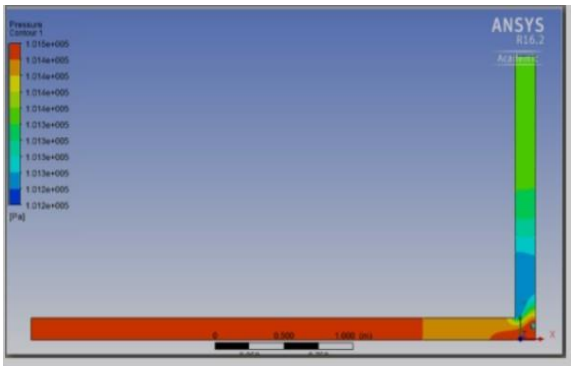

Fig. 9. Contour plot of pressure distribution for no turning vane.

From the Fig. 8 and Table 11 the separation length decreases as the number of vanes is increased. This reduction in separation length shows that the strength of the recirculation zone is reduced, and the flow tends to recover to become fully developed by the time it reaches the exit plane. Figures 9 to 11 present the total pressure contours inside the duct. It can be seen from Fig 8 that the pressure is very high in sharp corner of the elbow. The fluid velocity is low in this corner due to the presence of the separation zone. This will be the location that will break in case of wear-out. From the Figs 10 to 12, one can see that the pressure in the corner of the elbow is gradually reduced as the number of vanes is increased.

4.6. Influence of turbulence models

Simulations are performed using the standard k-ε and the k-ω turbulence models for the prediction of pressure loss.

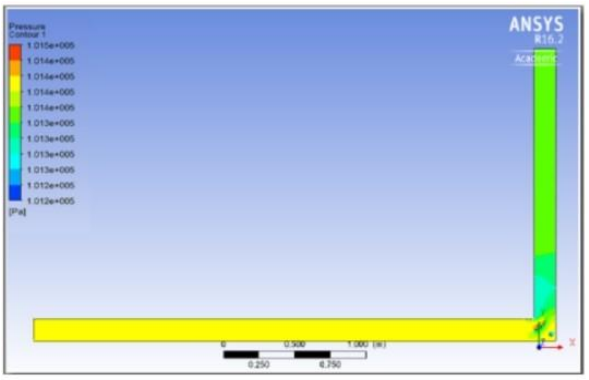

Fig. 10. Contour plot of pressure distribution for one turning vane(H=0mm).

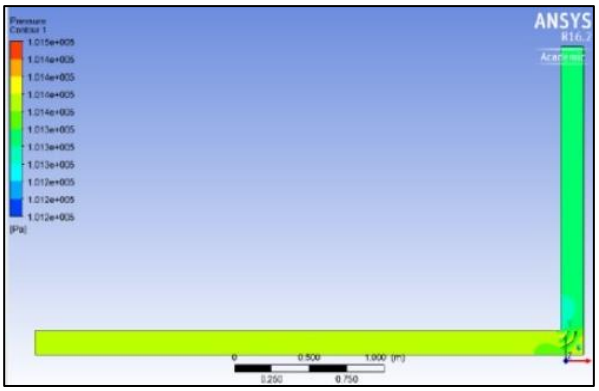

Fig. 11. Contour plot of pressure distribution for two turning vanes (H=0mm).

The turning vane of thickness of 1 mm and a fixed size of H=0mm was used for all vanes to study the influence of two turbulence models. Figure 13 shows comparison of results of performance between the standard k-ε and the k-ω turbulence models in predicting the pressure loss for various number of vanes. The number of vanes were changed from 0(no vane) to 3. The pressure losses predicted by the k-ε turbulence model is slightly higher compared to k-ω turbulence model prediction. From the above results and discussion, it can be concluded that the turning vanes can reduce the pressure loss. Pressure loss value is reduced if one turning vane is used. However, if more than one turning vanes are used, the pressure loss value starts increasing reducing the benefit of having turning vanes gradually. One possible reason for the reduced benefit as the number of vanes is increased could be that as the number of vanes is increased, the total surface area is increased. This increase in surface area will increase the skin friction adding to the pressure loss value. When the vane is fixed exactly at the elbow(H=0mm), the pressure loss value is significantly reduced. If the vane length is increased, the pressure loss value starts increasing.

From the above discussions the pressure loss value starts increasing as the vane length is increased. When the vane is fixed exactly at the elbow (H=0mm), the pressure loss value is significantly reduced. If the vane length is increased, the pressure loss value starts increasing. The improved performance of the duct with sharp bend in the presence of vanes may be due to the reduction in the width to depth ratio in the inner regions of the elbow, resulting in a significant reduction of the strength of secondary flow. Flow becomes more and more uniform both in the bend and in the region downstream of the elbow in the duct due to the presence of vanes. Sharp bends have been generally avoided by the engineers and contractors to eliminate or reduce the severe secondary flows and strong recirculation regions. The present study shows that the turning vanes can be used to reduce the adverse impacts of sharp elbows. When the vane is fixed exactly at the elbow(H=0mm), the pressure loss value is significantly reduced. If the vane length is increased, the pressure loss value starts increasing.

4.7. Effect of turning vane on the velocity profile at the outlet

Figures 14 to 17 display the velocity profiles close to the boundary outlet in configurations of turning vanes, H=0mm. Velocity profiles at the outlet computed with k-ε turbulence model are presented here. From the graph presented in Figs 14 to 17, we can see that as the number of turning vanes increase, the shape becomes parabolic. The flow at the end of the duct is tending to become fully developed as the numbers of vanes are increased. Basically, the flow tends to become more uniform like the flow in a straight duct.

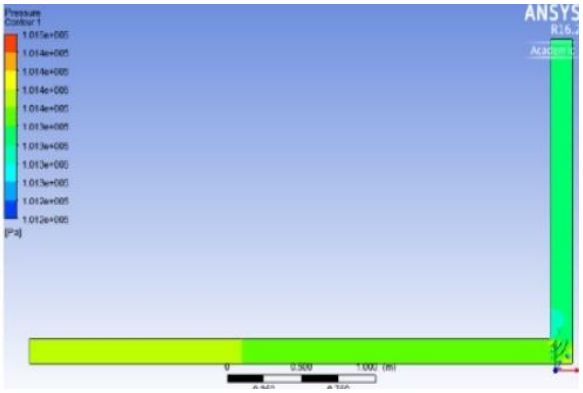

Fig. 12. Contour plot of pressure distribution for three turning vanes (H = 0 mm).

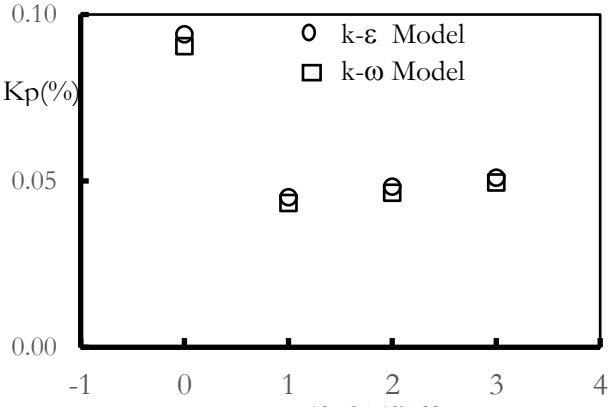

Fig. 13. Pressure loss with two turbulence models.

In summary, the present computational study shows that the turning vanes do reduce the pressure

loss in the duct with a 90˚ sharp elbow bend. There is a significant reduction in pressure loss when single vane with H=0mm (H/D=0) is used. If the vane length is increased beyond H=0mm (H/D=0), predicted pressure loss starts to increase. If the length of the turning vane is increased further, the pressure loss starts to increase. This increase in pressure loss continues up to a vane length of 400mm (H/D=2.66) up to which present studies were carried out. This increase in pressure loss for longer turning vanes could be due to skin friction on the turning vanes themselves which contribute to the pressure loss thus reducing the benefit due to presence of turning vane. It should be remembered here that these results show how that the single turning vane provides pressure loss benefits for various vane lengths.

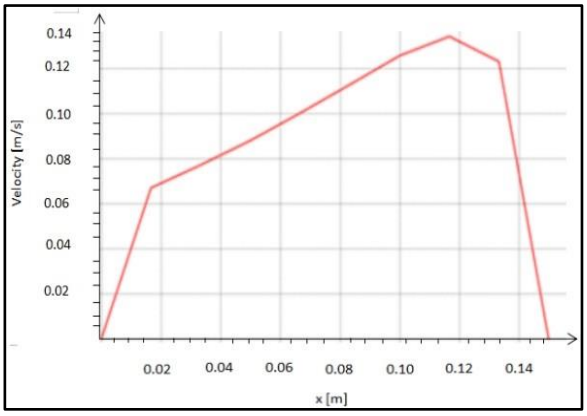

Fig.14. Velocity profiles close to the outlet for no turning vane.

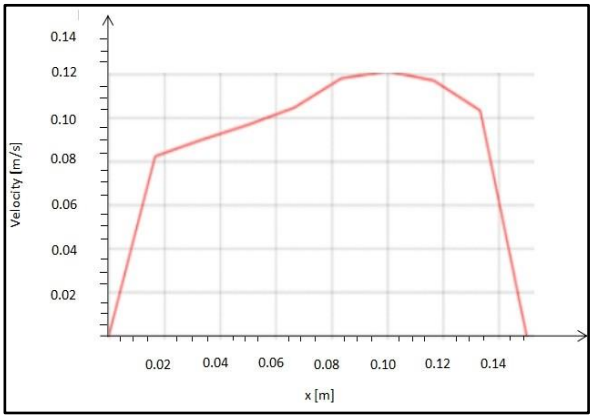

Fig. 15. Velocity profiles close to the outlet for one turning vane (H=0mm , H/D=0).

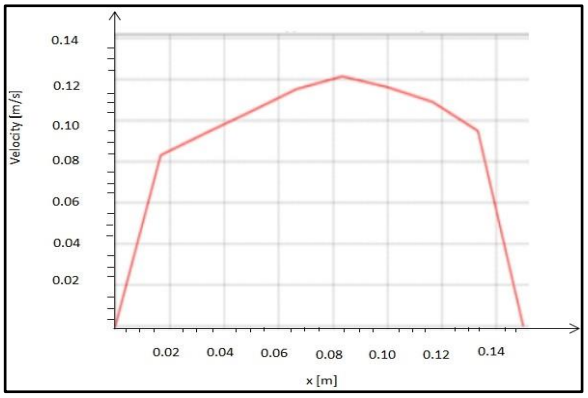

Fig. 16. Velocity profiles close to the outlet for two turning vane (H=0mm, H/D=0).

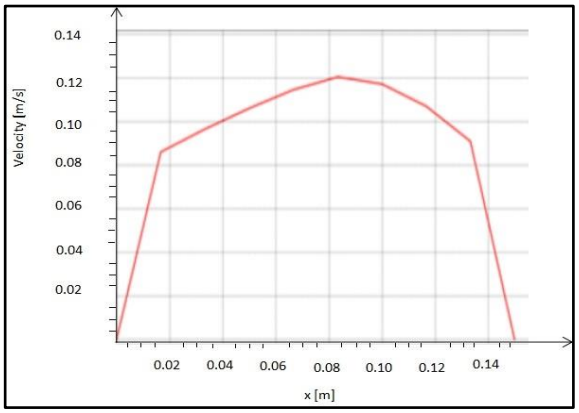

Fig. 17. Velocity profiles close to the outlet for three turning vane (H=0mm, H/D=0).

5 Conclusion

Numerical predictions of turbulent air flow inside a sharp horizontal-to-vertical 90˚ elbow are presented. Both the standard k-ε and the standard k-ω turbulence models were used in this study However, most of the results are presented using the standard k-ε turbulence model calculations. Available experimental data have been used to validate the initial computational model and numerical method. The computed results showed reasonable agreement with experimental data. The current study has been extended to calculate the pressure loss in the presence of turning vanes. The current numerical study shows that one turning vane, fixed at the middle of the duct in the bend, can reduce the pressure loss significantly. The pressure loss does not reduce if the vane length is increased beyond H=0mm(H/D=0). If the vane length is increased beyond H=0mm(H/D=0), the predicted pressure loss starts increasing, thereby reducing the benefit. The increase in pressure loss with increased vane length is suspected to be because of the increased contribution of skin friction from the turning vanes

themselves. The present computational study shows that the multiple turning vanes are effective in reducing the pressure loss in a duct with a 90˚ sharp elbow. As the number of turning vanes are increased, the pressure loss also increases. If the lengths of all turning vanes are extended on both sides from 100mm to 400mm in steps of 100mm (H/D=0, 0.66, 1.25, 2 and 2.66) then pressure loss is increased thereby reducing the benefit. For multiple vanes of length other than H=0mm, the pressure loss is increased and this could be because of the skin friction on the turning vanes themselves which contribute to the pressure loss thus reducing the benefit due to the presence of turning vanes. The velocity profiles tend to become more developed as the number of vanes is increased, significantly reducing the asymmetry in the velocity profile at the outlet. As far as the pressure loss is concerned, the optimum extension length of H=0mm (H/D=0) and one vane seems to perform better than other configurations. It should be noted here that H=0mm means that the vane is not extended on either side into the straight section. Separation length on the left vertical wall reduces as the number of vanes is increased. The performances of both the turbulence models were not significantly different from each other in the prediction of pressure loss in the duct with and without turning vanes. The improved performance of ducts with bends in the presence of turning vanes may be attributed to the fact that there is a reduction in the ratio of width to depth in the different inner regions of the elbow. This results in more flow recovery to take place both in the elbow and in the region beyond the elbow in the duct due to the presence of vanes. The current study shows mathematically that turning vanes can be used to reduce the adverse effect of sharp elbows on pressure loss.

Acknowledgment

The authors would like to thank the support rendered by the Department of Mathematics and Statistical Sciences and the Botswana International University of Science and Technology, Palapye, Botswana.

References:

[1] P. S. Klebanoff,"Characteristics of turbulence in a boundary layer with zero pressure gradient", NACA TN 3178,1954.

[2] H. Ito, K. Imai,"Pressure losses in vaned elbows of a circular cross section", Transactions of the ASME, Series D, pp 684-685,1966.

[3] L. B. Ellis, P. N. Joubert, "Turbulent shear flow in a curved duct", *Journal of Fluid Mechanics*, Vol.62,1974, pp.65-84.

[4] I. A. Hunt, P. N. Joubert, "Effects of small streamline curvature on turbulent duct flow", *Journal of Fluid Mechanics*, Vol.91, 1979, pp.633-659.

[5] J. A. C. Humphrey, J.H. Whitelaw, G. Yee," Turbulent flow in a Square Duct with Strong Curvature", *Journal of Fluid Mechanics*, Vol.103,1981, pp.443-463.

[6] S. S. Han, A. S. Ramamurthy, P. M. Biron, "Characteristics of Flow around Open Channel 90° Bends with Vanes ", *Journal of Irrigation and Drainage Engineering,* Vol.137, No.10. pp. 668-676, 2011, ISSN 0733-9437.

[7] W. Stafford, "An Investigation of Flow in Circular and Annular 90-degree Bends with a Transition in Cross Section", NACA TN 3995, 1957.

[8] J. Henry, R. John, "Design of Power-Plant Installations. Pressure-Loss Characteristics of Duct Components", NACA WR L-208,1944.

[9] E. Floyd, "Investigation to Determine Effects of Rectangular Vortex Generators on the Static-Pressure Drop Through a 90-degree Circular Elbow", NACA RM L5508,1953.

[10] R. Mossad, W. Yang, M.P. Schwarz, "Numerical prediction of Air Flow In a sharp 90 degree Elbow", 7th International Conference on CFD in the Minerals and Process Industries, CSIRO, Melbourne, Australia, 9-11, Dec 2009.

[11] S. F. Sanchez, J. R. Luna, M. I. Carvajal, R. E. Tolentino," Pressure Drop Models Evaluation for Two-Phase Flow in 90 Degree Horizontal Elbows", *Ingeniería mecánica, tecnología y Desarrollo,* Vol. 3, 2010, pp. 115-122.

[12] Benbella S., Al-Shannag, and Al-Anber Z. A., "Gas-liquid pressure drop in vertical internally wavy 90-degree bend ", *Experimental thermal and Fluid Sciences*, vol. 33, No. 2, 2009.

[13] A. M. K. P. Taylor, J. H. Whitelaw, M. Ylanneskis, "Curved ducts with strong secondary motion: velocity measurements of developing laminar and turbulent flow", *Journal of Fluids Engineering*, Vol.104, pp. 350-359,1982.

[14] A. Yilmaz, E.K. Levy, "Formation and Dispersion of ropes in pneumatic conveying", *Powder Technology*, Vol.114, 2001, pp.165-185.

[15] M. M. Klazly, G. Bognar, "CFD Study for the Flow Behaviour of Nanofluid Flow over Flat Plate", International Journal of Mechanics, Vol.14, No. 22, 2020, pp. 49-57.

[16] G. Cannata, F. Gallerano, F. Palleschi, C. Petrelli, L. Barsi," Three-Dimensional Numerical Simulation of the Velocity Fields

Induced by Submerged Breakwaters", International Journal of Mechanics, Vol.13, 2019, pp. 1-14.
[17] S. A. Mumma, T.A. Mahank, Yu-Pei Ke, "Analytical determination of duct fitting loss-coefficients", *Applied Energy*, Vol.61, 1998, pp.229-247.
[18] A. M. Chan, K. J. Maynard, J. Ramundi, E. Wiklund,"Qualifying elbow meters for high pressure flow measurement in an operating nuclear power plan ", Miami, Fl, USA, 2006.
[19] A. Azzi, L. Friedel, "Two-phase upward flow 90 bend pressure loss model", vol.69, No.2, 2005.
[20] S. K. Wang, "Handbook of Air Conditioning and Refrigeration", 2nd edition, 2001.
[21] I. E. Idelchik, "Handbook of Hydraulic Resistance ", Begell House, 1994.
[22] L. Murthy, J. Cui," Numerical investigation of pressure loss reduction in a power plant stack", *Applied Mathematical Modelling*, Vol.31, 2007, pp.1915-1933.
[23] K. Langwane, N. Subaschandar, "Pressure loss reduction in a duct with a 90-degree sharp elbow using a turning vane." Presented at the International conference SAMSA 2018, Southern African Mathematical Sciences Association, Botswana, Nov 19-22, 2018.
[24] Ansys Workbench Student Version, Ansys® Academic Research Mechanical, Release 16.2 Help System, Coupled Field Analysis Guide, 2016.
[25] F.M. White, Fluid Mechanics, New York, McGraw-Hill publications, USA, 2011.
[26] S. V. Patankar, "A calculation procedure for two-dimensional elliptic situations", *Numerical Heat Transfer*, Vol.4, No.4, 1981, pp. 409-425.
[27] B E. Launder, D. B. Spalding, Mathematical models of turbulence, Academic Press, Waltham, U.K, 1972.
[28] B. E. Launder, D. B. Spalding," The numerical computation of turbulent flows", *Computer Methods in Applied Mechanics and Engineering*, Vol. 3, 1974, pp. 269–289.
[29] D. C. Wilcox, "A complete model for turbulence", AIAA Paper No.84-0176, 1984, Reno, Nevada, USA.
[30] D. C. Wilcox, Turbulence modelling for CFD, ISBN 1-928729-10-X, 1988, 2nd Ed, DWC Industries, Inc La Canada, California, USA.
[31] S. V. Patankar, Numerical Heat Transfer and Fluid Flow. Taylor & Francis, 1980, ISBN 978-0-89116-522-4.
[32] J. Solórzano-López, R. Zenit, M. A. Ramírez-Argáez,"Mathematical and physical simulation of the interaction between a gas jet and a liquid free surface", *Applied Mathematical Modelling*, Vol.35, No.10, 2011, pp.4991-5005, ISSN 0307-904X.
[33] W. Yang, B. Kuan,"Experimental investigation of dilute turbulent particulate flow inside a curved 90o bend", Chemical Engineering Science, Vol. 61, 2006, pp 3593–3601.
[34] P. K. Vijayan, A.K. Nayak, N. Kumar, "Chapter 3-Governing differential equations for natural circulation systems", Single-Phase, Two-Phase and Supercritical Natural Circulation Systems, Eds: P. K. Vijayan, A. K. Nayak, N. Kumar, Woodhead Publishing, 2019, pp.69-118, ISBN 9780081024867.

Author Contributions: Please, indicate the role and the contribution of each author:

N. Subaschandar gave the idea, formulated the problem, supervised the work, and contributed a lot in writing the manuscript.

K. Langwane carried out all the simulation work

Sources of funding for research presented in a scientific article or scientific article itself

The research reported in this paper was not funded by any agency. It was not funded by the University or the Department.